INSTITUT DE FRANCE
Académie des sciences

Comptes Rendus
Physique

Xiaomeng Zhang, Benfeng Bai and Hong-Bo Sun

Dispersion and efficiency engineering of metasurfaces

Volume 21, issue 7-8 (2020), p. 641-657

Published online: 3 November 2020
Issue date: 19 January 2021

https://doi.org/10.5802/crphys.18

Part of Special Issue: Metamaterials 2
Guest editors: Boris Gralak (CNRS, Institut Fresnel, Marseille, France) and Sébastien Guenneau (UMI2004 Abraham de Moivre, CNRS-Imperial College, London, UK)

This article is licensed under the
Creative Commons Attribution 4.0 International License.
http://creativecommons.org/licenses/by/4.0/

Les Comptes Rendus. Physique *sont membres du Centre Mersenne pour l'édition scientifique ouverte*
www.centre-mersenne.org
e-ISSN : 1878-1535

Comptes Rendus
Physique
2020, 21, nº 7-8, p. 641-657
https://doi.org/10.5802/crphys.18

Metamaterials 2 / *Métamatériaux 2*

Dispersion and efficiency engineering of metasurfaces

Ingénierie de la dispersion et de l'efficacité des méta-surfaces

Xiaomeng Zhang [a], Benfeng Bai [*, a] and Hong-Bo Sun [a]

[a] State Key Laboratory of Precision Measurement Technology and Instruments, Department of Precision Instrument, Tsinghua University, Beijing, China

E-mails: zhangxm16@mails.tsinghua.edu.cn (X. Zhang), baibenfeng@mail.tsinghua.edu.cn (B. Bai), hbsun@mail.tsinghua.edu.cn (H.-B. Sun)

Abstract. Metasurfaces, ultrathin two-dimensional arrays of artificially engineered meta-atoms, can impart spatially varying changes towards the incident electromagnetic wave and provide versatile functionalities once unprecedented in sub-wavelength thick natural materials. The wavefront manipulation by metasurfaces usually arises from the strong resonant behaviors of varied meta-atoms in subwavelength lattice, which also brings some drawbacks like the unexpected dispersion due to separate resonances of the meta-atoms and the long concerned low efficiency problem. This paper reviews the recent surge of fruitful works on dispersion and efficiency engineering of metasurfaces and provides an overview of several effective methods to acquire metasurfaces with these distinctive features.

Résumé. Les méta-surfaces, des réseaux bi-dimensionnels ultra-fins de méta-atomes artificiels, peuvent transférer les variations spatiales de leur structure au champ électromagnétique et conférer ainsi des fonctionnalités jusqu'alors inégalées dans les matériaux naturels d'épaisseur sous-longueur d'onde. La manipulation du front d'onde par les méta-surfaces est généralement obtenue en exploitant le caractère fortement résonant des méta-atomes dans le réseau sous-longueur d'onde, qui conduit par ailleurs à des inconvénients tels qu'une dispersion inattendue en raison des résonances distinctes des méta-atomes et un problème d'efficacité qui a fait l'objet d'une attention de longue date. Cet article passe en revue les percées récentes des travaux sur ces problématiques de la dispersion et de l'efficacité des méta-surfaces et il donne un aperçu de plusieurs méthodes permettant d'obtenir des méta-surfaces avec des propriétés remarquables.

Keywords. Metasurface, Bound state in the continuum, Dispersion engineering, Material, Efficiency.

Mots-clés. Métasurface, État lié dans le continuum, Ingénierie de dispersion, Matériel, Efficacité.

2020 Mathematics Subject Classification. 00-01, 99-00.

Available online 26th November 2020

* Corresponding author.

1. Introduction

Manipulating electromagnetic waves at will has long been a pursued goal since the establishment of electromagnetism. Numerous efforts have been made in this field and have brought abundant achievements in many areas, such as communication, energy, and entertainments. By applying electromagnetic field to a material, electric and magnetic responses are induced by the properties of the material, i.e. permittivity and permeability, which incur specific manipulation to the incident field. For natural materials, these properties have limited range in different frequency domains, which naturally set a limitation to the capability of engineering the field [1].

Metamaterials are a kind of artificial materials that can overcome the aforementioned impediment. This feature comes from its subwavelength artificial compositions, called meta-atoms. Permittivity and permeability describe the averaging polarized fields over a domain that occupies an area much larger than atom but smaller than wavelength. For natural materials, the composition over this domain is homogeneous. While metamaterials enable different geometries of meta-atoms in this domain, which may generate various artificial effective permittivity and permeability related not only to material but also to the geometry [2]. By means of this new paradigm, a lot of new phenomena have emerged, such as negative index [3], hyperbolic dispersion [4] and invisibility cloak [5]. However, the fabrication of three-dimensional subwavelength structures is quite challenging and the high loss due to the propagation in the material also hinders its potential applications.

In recent years, a type of ultra-thin planar metamaterials, called metasurfaces [6], are proposed to overcome these problems. Metasurfaces can exploit the well-developed standard semiconductor fabrication process and is easy to integrate due to its ultra-thin trait. Although metasurfaces are lack of field transformation in the direction along propagation, they can impart various manipulations to the incident field [7] and have been utilized to achieve control of many properties of light including the amplitude [8], frequency [9], phase [10], polarization [11] and momentum [12]. Despite the similar constructions of metamaterials and metasurfaces, they have essential differences [13]. The manipulation of field in metamaterials still relies on the optical path accumulation during propagation; while for metasurfaces, as its interactive length with field is extremely thin, the changes it imparts to the field can be seen as abrupt ones. Therefore, instead of concerning the bulk properties of metasurfaces, we can regard the metasurfaces as zero-thickness interfaces [14], whose surface susceptibilities or impedances are of great importance. By deliberately choosing the materials and geometries of the meta-atoms, metasurfaces may enable spatial-variant and multimode interactions [15], serving as efficient platforms for manipulating electromagnetic waves.

In order to obtain useful functionalities with metasurfaces, the meta-atoms need to interact strongly with the incident field, imparting a scattering field with a large difference from the incident one. This resonant state of meta-atom, however, often brings some drawbacks. The scattering spectrum of a single resonator is often represented by a Lorentzian curve [16] in the frequency domain, with the phase delay changing from 0 to π near the resonance. The width of the curve is related to the losses both from absorption and radiation. For an opening resonator and a continuum mode, this resonance width often lays in a certain range, so that the working wavelength of a metasurface can be neither too broad nor too narrow and the dispersion of a metasurface is also limited. This trait needs to be engineered for specific applications. For example, sharper resonances are preferred in ultra-highly sensitive sensing [16], field modulation [17] and nonlinear interactions [18]; while smoothly varied resonances are preferred in full-color imaging [19], holographic display [20] and other broadband applications. Hence, the dispersion of metasurfaces should be carefully engineered concerning specific applications in the interested frequency ranges. Besides, the power utilization efficiency of metasurfaces is also of great im-

portance. From the earlier plasmonic structures working under cross-polarized condition with a maximal efficiency under 25% [21], the exploration in this field ranges from optimization of the materials [22] and the interference of different multipoles to match the impedance utterly, aiming to achieve 100% efficiency that is highly desired in many realistic applications. This requirement gets harsh when it comes to the gradient metasurfaces [23] to reroute all the power into the desired direction, where the impedance boundary condition has to be carefully satisfied to obtain perfect wave manipulation with unitary efficiency.

In this review, we have an overview on recent endeavors in solving the aforementioned limitations of metasurfaces. First, we review the ways of engineering the dispersion of metasurfaces, achieving either sharp resonances with high quality factors or smooth resonances working under broadband wavelength range. Then, the works exploring high efficiency metasurfaces are reviewed from both material and structural perspectives, by discussing the features of the structures that can achieve nearly unitary efficiency in both periodic and gradient quasi-periodic arrangements.

2. Dispersion engineering of metasurfaces

2.1. *Highly dispersive metasurfaces*

Highly dispersive metasurfaces, with strong resonances of high quality factors, have great importance in applications such as sensors, modulators like optical switches, slow-light devices [24] and nonlinear devices. To obtain such resonances, Fano resonance [25] with steep dispersion is usually exploited, which originates from the coupling between a discrete localized state and a continuum state.

Since the observation of an unusual sharp asymmetric line in the absorption spectra of noble gas, this resonance, bearing its explainer's name Fano, has attracted a lot of attentions due to its distinctive difference from the conventional Lorentzian resonance curve. This phenomenon was first discovered and explained in a quantum mechanical study of photoionization of atom [26]. The photoionization can go along two channels [27], direct ionization and autoionization, where the atom transits from the ground state to a continuum state directly or with an intermediate autoionization state, respectively. Fano resonance profile appears because of the interference between these two different paths. Among these two paths, intermediate autoionization state is of great importance. The autoionization state is a quasi-bound state and corresponds to a resonance with finite lifetime in scattering. This quasi-bound state can be regarded as the result of coupling between the bound state from one channel and the continuum state from the other channel. Hence, the coupling between a bound state and a continuum state is essential to obtain the so-called Fano resonance.

The formula for the scattering cross-section curve of Fano resonance with no absorption loss is expressed as [28]

$$\alpha = \frac{2\pi}{E(1+q^2)} \frac{(\Omega+q)^2}{1+\Omega^2}, \tag{1}$$

where E is the energy, Ω is defined by $2(E-E_F)/\Gamma$, q is the so-called Fano parameter (which is the ratio of the transition probabilities to the continuum state intermediately and directly), and E_F and Γ are the resonant energy and the width of the autoionization state, respectively. Equation (1) is applicable when the width of the resonance corresponding to this quasi-bound state is narrower enough than those of other resonances. According to (1), the curve has a minimum at $E = E_F - \Gamma q/2$ and a maximum at $E = E_F + \Gamma/(2q)$ and owns an asymmetric feature when q is neither 0 or infinity. This phenomenon appears when the scattering field corresponding to the autoionization undergoes a sharp phase change of π at the resonance, so

that there will be constructive and destructive interferences between the two different paths, which can be located extremely close with an interval as $(q + 1/q)\Gamma/2$. This sharp variation from maximum to minimum in the profile could happen in a width nearly equal to that of the quasi-bound state, when the transition of the two paths are of the same strength, as shown in Figure 1(a).

There is another interesting discovery called bound state in the continuum (BIC) [29] in quantum system that also concerns the extremely high quality factor of the resonance. BIC is an exact bound state inside the continuum state and remains perfectly confined, which completely decouples with the radiating waves. It is quite different from the autoionization state in Fano resonance. In this sense, BIC can be regarded as a resonance with zero linewidth and infinitely high quality factor, which can only exist in structures with uniformity or periodicity in at least one dimensions to ensure the utter localization of the bound state. By considering the limited sample size and fabrication imperfections, the rigorous criteria on BIC make its practical realization impossible. But inspired by the requirements on BIC, a quasi-BIC with finite but quite high quality factor can be achieved, which can often be fulfilled by imparting a little perturbation to the ideal BIC system to turn the bound state in continuum into a leaky resonance. Recently, there is rigorous demonstration linking the transmission/reflection profile of quasi-BIC to the exact Fano formula [30], where the Fano parameter becomes ill-defined and the profile loses the features of Fano asymmetry. Thus, Fano resonance can be seen as a harbinger of BIC. Suppression of coupling between the bound state and the continuum state by tuning the parameter of structures or excitation conditions can transform them from one to the other.

Having the inspirations from Fano resonance and BIC in quantum systems, we focus on these phenomena in metasurfaces interacting with electromagnetic waves where interference is also ubiquitous. Metasurfaces provide particular platforms to obtain these phenomena, as they may support resonances of large diversity and favor experimental feasibility. Generally, the realization of BIC in mertasurfaces can be divided into three classes: symmetry protecting, total destructive interference of two resonances in the same cavity, and total destructive interference among different radiation channels. By introducing perturbations in these situations, quasi-BIC with Fano profile and high quality factor can be obtained.

The most prevalent method is through symmetry protecting. The complete prohibition of the outcoupling of the bound state can be realized by building different symmetry classes between the bound state and the continuum state. As the modes of different symmetry classes can be completely decoupled, this kind of symmetry-protected BIC can be quite robust even with varied structural parameters as long as the symmetry is not broken. Quasi-BIC originating from this symmetry-protected BIC comes from the slight breaking of the symmetry of the bound state, which directly results in its coupling with the continuum state. A resonance featured with Fano profile emerges, and moreover, its quality factor is directly related to the extent of symmetry breaking [30, 34]. Symmetry breaking relies on either the structures [35] or excitation conditions [36]. Considering different symmetry traits of different bound states, both in-plane [37–39] and out-of-plane symmetry [40] breaking have been explored. With the appropriate parameter tuning towards the critical point of symmetry, the change of quality factor from finity to infinity can be observed. In this way, quasi-BIC with extremely high quality factor can be acquired. Recently, with the help of a metasurface with subwavelength period of rod dimers varied from detuned to tuned, a transition from quasi-BIC to BIC was clearly exhibited [31], as shown in Figure 1(b). A coupled dipole analysis shows that the dimers support both symmetric and asymmetric modes. When the rod dimers are identical, the asymmetric mode is completely suppressed, which leads to symmetry-protected BIC with infinite quality factor. When the dimers are detuned, i.e. the dimers are different in geometry, the asymmetric mode turns into a leaky mode and the interference between symmetric and asymmetric mode contributes to the typical Fano profile in

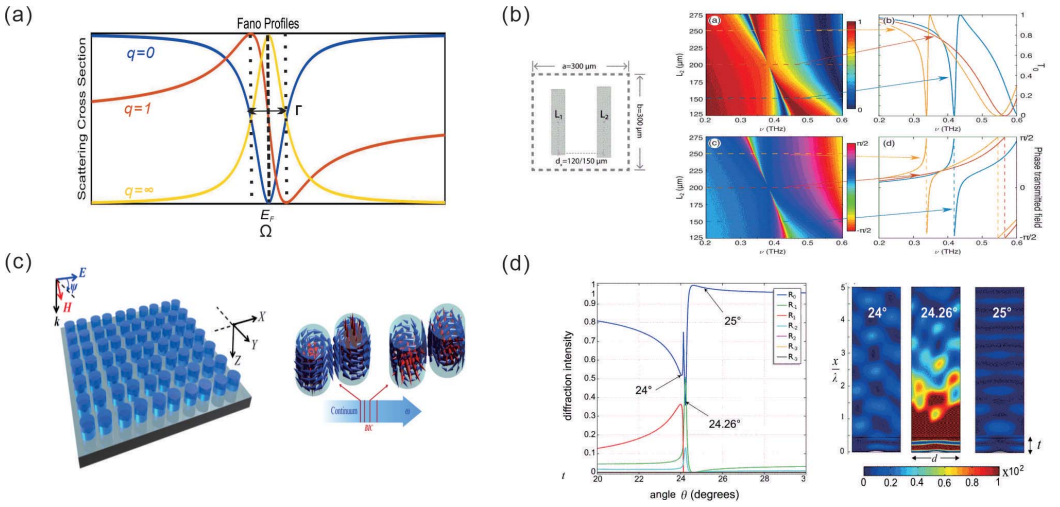

Figure 1. (a) The Fano profiles of different q. $q = 0$ corresponds to anti-resonance, $q = \infty$ corresponds to normal Lorentz resonance and $q = 1$ corresponds to the largest dispersion. (b) Symmetry-protected BIC. With the dimers varing from detuned to tuned status, a transition from Fano resonance to BIC is clearly exhibited from the reflectance diagrams. Reprinted with permission from [31] © The Optical Society. (c) Symmetry protected and unprotected toroidal dipole BIC. BIC originated from total destructive interference of toriodal and electronic dipoles are symmetry unprotected and can maintain relatively high quality factors when the symmetry is broken. Adapt with permission from [32] © The American Physical Society. (d) Quasi-BIC originated from a little deviation from destructive interference of Rayleigh and resonance anomalies. With a slight variation in the incident angle, the field intensity distribution changes utterly, indicating a high quality factor of the resonance anomaly. Adapt with permission from [33] © The Institute of Physics.

the transmission spectrum. Zigzag arrays [41] can also fulfill quasi-BIC with high quality factor under the same formalism. By making the resonant frequency of the coupled continuum mode far away from that of the bound state, there is no resonant background for quasi-BIC, which has been desired in applications like filtering.

The second method is the total destructive interference between two resonances in the same cavity and radiating into the same radiation channel, which is also called the Friedrich–Wintgen BIC [42]. In temporal coupled-mode theory [43], with these two resonances tuned, the eigenvalues of the resonator, as a function of its certain geometrical parameter, come near to crossing but then repel each other in the complex plane. When there is an avoided resonance crossing [44], either for real or imaginative part of eigenvalue, an important feature is generated, i.e., a state with a considerably increased lifetime and a simultaneous state with short lifetime. In order to turn the state with increased lifetime into a BIC, the two tuned resonances need to be coupled predominately in the far field with vanishing near-field coupling [32, 45], as shown in Figure 1(c), or own almost the same radiation rates [46]. Metasurfaces supporting this kind of BIC own some advantages compared to symmetry-protected BIC. As the divergence of the incident angle cannot be prevented in practical scene, the symmetry class of metasurface and its excitation condition cannot be pure. Thus, for a given quality factor, metasurfaces with Friedich–Wintgen BIC can achieve a smaller footprint than that of symmetry-protected BIC.

The third method for obtaining BIC needs only one resonance and the complete radiation vanishing comes from the destructive interference from two or more different radiation channels.

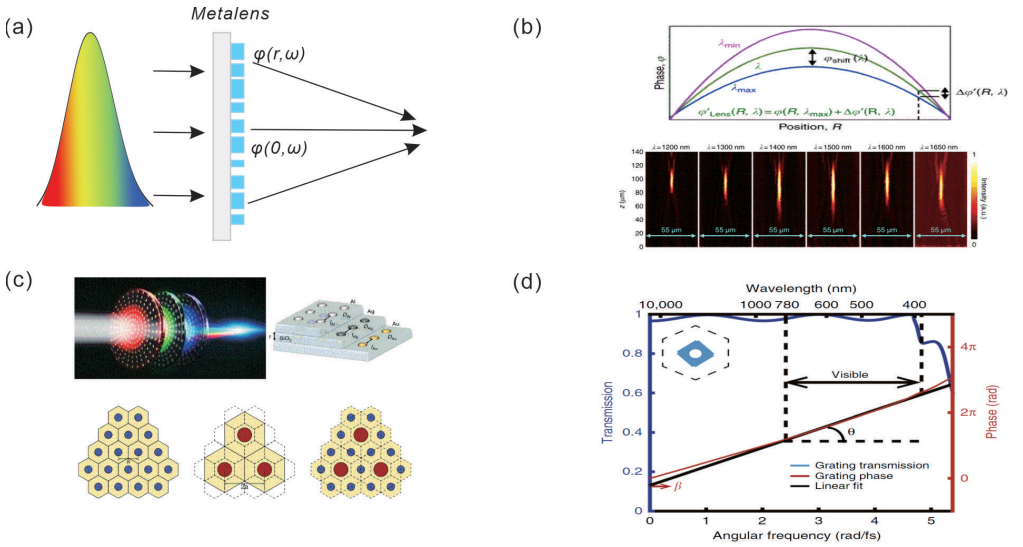

Figure 2. (a) A metalens without chromatic dispersion requires additional engineering of group delay, in order to maintain the identical shape of the incident pulse. (b) Achromatic focusing requires the phase delay profiles to change with the incident frequency. Adapted with permission from [47] © Springer Nature. (c) A stacked multilayer metasurface and an interleaved metasurface. Adapted with permission from [48] and [49] © Springer Nature. (d) The engineered dispersion of the resonator, which can offer the desired group delay with high efficiency. Reprinted with permission from [50] © Springer Nature.

A reflective grating with an extreme form of Wood's anomalies can support resonances with diverging quality factor [33]. This extreme form exists when two kinds of Wood's anomalies, i.e. Rayleigh anomaly and resonance anomaly, merge. Rayleigh anomaly occurs when a diffraction order emerges or vanishes, while resonance anomaly occurs when a diffraction order exciting the guided mode that the grating supports. The merge of these anomalies can be obtained by tuning the incident angle together and the period. This kind of BIC can be understood in the framework of leaky wave theory and can obtain quasi-BIC with relatively high quality factor in the vicinity of the critical tuning, as shown in Figure 1(d).

2.2. *Smoothly dispersive metasurface*

Metasurfaces with ordinary Lorentzian resonances often exhibit a dispersion changing too swiftly for broadband applications, due to the periodic lattice as diffractive device and the composed resonant meta-atoms. For a resonant meta-atom, its scattering field (both amplitude and phase) may undergo a large dynamic range near its resonance frequency. Although for some metasurfaces, whose phase profile is enabled by Pancharatnam–Berry (PB) phase [51], can provide exactly the same phase transformation to the incident field of different frequency, the amplitude cannot be held and the chromatic dispersion due to phase accumulation during the propagation of light cannot be eliminated. For this reason, most metasurfaces are designed under a particular working wavelength and usually exhibit negative chromatic dispersion [52] in the limited adjacent spectral range. Metasurfaces with smooth dispersion are especially desired for various applications in color imaging and display, such as the elimination of chromatic dispersion, where meta-atoms should impart smoothly varied phase delay at different frequencies to compensate

the phase difference arising from propagation. Taking broadband metalens as an example, the phase delay should be engineered as [53]

$$\varphi(r,\omega) = \frac{\omega}{c}\left(-\sqrt{r^2+f^2}+f+\alpha\right)+\beta, \tag{2}$$

where ω is the angular frequency, r is the location on the metasurface, c is the light velocity, f is the focal length of the meta-lens, α is the spatial phase reference and β is the spectral phase reference. This equation can be directly get considering the Fermat principle in the scene depicted in Figure 2(a). When the angular frequency changes, the phase delay profile changes accordingly, as shown in Figure 2(b). Meta-atoms, which can accomplish the local phase delay defined by (3), impart different phase delays towards the impinging field of different frequency and can be immune from chromatic dispersion.

Eliminating chromatic dispersion at several discrete wavelengths were first addressed using metasurfaces, as shown in Figure 2(c). Stacked multilayer metasurfaces [48] are kind of approach conceptually simple yet powerful. Each layer is designed for one particular wavelength and the spectral crosstalk between each layer are set to be minimal. Interleaved metasurfaces [49] as another approach take a similar strategy. This aperture-shared method allows several metasurfaces designed for discrete wavelengths to assemble a hybrid single-layer metasurface. Comparing these two methods, the stacked metasurfaces allow meta-atoms of different materials for each layer, so that they can have lower crosstalk and higher efficiency. Instead of composing several ordinary metasurfaces together, there are also some endeavors of trying to engineer the dispersion at discrete frequencies of meta-atoms [54–56], so that they can naturally compensate the phase due to chromatic dispersion.

When it comes to continuous wavelength, wave manipulation enabled by metasurfaces without chromatic dispersion calls for more characteristics. Here we consider (3) again and get the derivative of φ with respected to ω,

$$\frac{\mathrm{d}\varphi(r,\omega)}{\mathrm{d}\omega} = \frac{1}{c}\left(-\sqrt{r^2+f^2}+f+\alpha\right), \tag{3}$$

which indicates that the structures we need in the metalens without chromatic dispersion should have certain group delay in their working wavelength range. And the absolute value of the group delay becomes larger with the positions of structures becoming farther from the center, which definitely sets limitations to the metalens on its working wavelength range and aperture. The device satisfying these requirements has shown exciting results especially on color imaging. Among them, achromatic metalens in the visible region from 400 nm to 660 nm with a numerical aperture (NA) of 0.106 in transmission mode was realized [57]. For plasmonic meta-atoms, large phase compensation can be achieved by adding more resonators in one unit cell [47]. With achromatic PB phase as the basic phase, the meta-atoms are deliberately designed, so that their own resonances compensate the phase differences arising from achromatic aberration and satisfy the group delay requirements. For dielectric meta-atoms, this method also works. While the field is usually localized inside the dielectric resonators, using field coupling among the dielectric resonators may not be as efficient as their plasmonic counterparts when compensating this phase difference. Therefore, resonators supporting higher multipoles [58] can be employed to achieve this goal. Using pillars with holes as the basic structures, 400 nm-thick silicon nitride structures can have outstanding dispersion properties [50], as shown in Figure 2(d). No matter what kind of meta-atoms are used, the selection of meta-atoms is a nontrivial job to assure the meta-atoms to offer the exact phase delays over the certain spectral range and suitable field intensity. Besides, when the working spectral range and the NA of the lens get larger, the requirement on the phase compensation becomes harsher and there would eventually be a tradeoff.

Generally, in order to have a smooth dispersion, meta-atoms are usually designed to support several modes. By tuning the parameters deliberately, these modes can work together to provide the required phase-frequency curves for different broadband applications.

3. Metasurfaces with high efficiency

Efficiency of metasurfaces has long been concerned for its importance in various device applications. Endeavors in this area ranges from the material choice to structural design, among which several methods, utilizing gap plasma resonance [59], Kerker effect [60] and waveguide-like resonance [61], have achieved great progress on metasurfaces with periodic meta-atoms. When metasurfaces come to a spatial-variant form, it calls for more delicate method to realize unitary efficiency, which is different from the common process of designing metasurfaces guided by the generalized Snell's Law [62]. Meta-gratings [63] and metasurfaces with spatial dispersion engineering [64] have been proposed to gain a higher efficiency for this kind of spatial-variant metasurfaces.

3.1. *Material choice of metasurfaces*

Meta-atoms made of noble metals, such as gold and silver, were first applied in metasurfaces due to its high conductivity and relatively low ohmic loss. The high conductivity makes the free electrons in meta-atoms strongly couple to the incident light and form the so-called local surface plasmon resonances [65]. This kind of resonances can increase the field density near the metal surfaces by orders of magnitude and localize the field into a sub-diffraction scale. But when the working wavelength comes to the near-infrared or visible range, the ohmic loss in metasurfaces severely increases because of the electron scattering and interband transitions [66]. Besides, noble metals are not compatible with the standard CMOS fabrication process (either chemical unstable or easily diffused) and cannot withstand high incident power or temperature. Considering these inherent drawbacks of noble metals, different materials have been explored to find the best substitution in near-infrared and visible frequency domain.

Materials, with comparatively large negative real part and relatively small imaginary part of permittivity compared to noble metals, are the best candidates to replace noble metals in plasmonic metasurfaces. However, nowadays alternatives of noble metals, like transparent conducting oxides (TCOs) and nitrides for near- or mid-infrared and visible spectral range [22, 67], can only obtain a tradeoff between these two requirements. TCOs can be heavily doped with a carrier concentration more than 10^{21} cm^{-3}, which is not possible for many semiconductors due to the solid-solubility limit. This carrier concentration guarantees the metallic feature of TCOs and a weaker electron scattering, together with a wide bandwidth that results in no inter-band loss. Hence, TCOs have much lower loss than noble metals at infrared frequency. However, the absolute value of the real part of their permittivity is much smaller than those of noble metals, as shown in Figure 3(a), indicating that noble metals still outperform TCOs for plasmonics [68]. The carrier concentration of typical metals can reach 10^{23} cm^{-3}, which results in a high plasma frequency and a high damping rate. Generally, TCOs can exhibit loss five times smaller than Ag in near-infrared frequency. Transition metal nitrides can be doped to an even higher carrier concentration as high as 10^{22} cm^{-3}, with the plasma frequency locating in the visible range similar to Au [69]. Transition metal nitrides are a kind of refractory materials with high chemical stability [70] and high damage threshold [71]. The loss in nitrides, however, are actually larger than that in bulk noble metals, due to both inter-band transition and Drude damping. For noble metals acquired upon evaporation, which are commonly used in plasmonic metasurfaces, the grain boundaries and roughness in metals cause additional scattering and result in higher loss. While

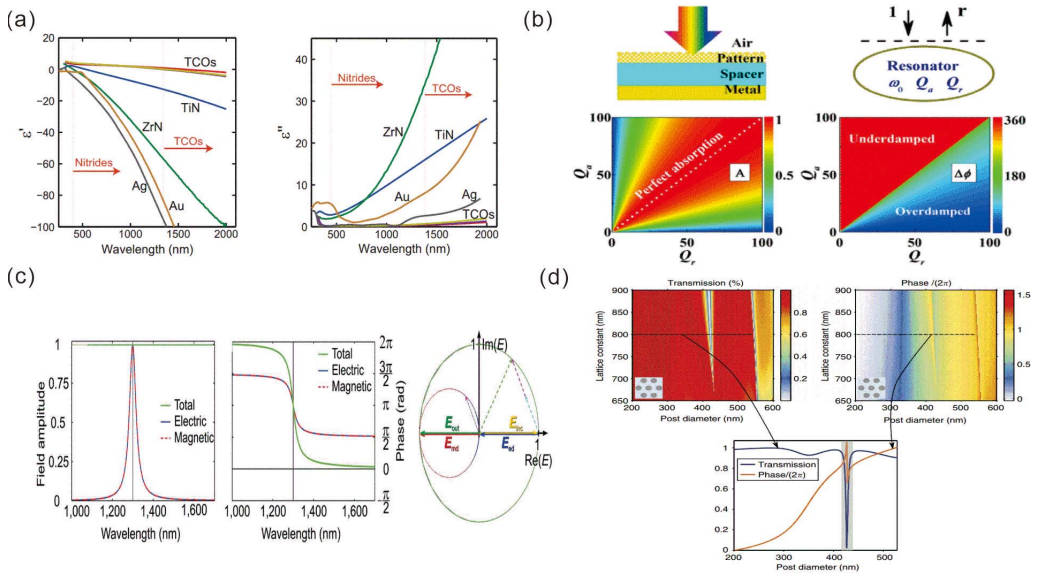

Figure 3. (a) Permittivity figures of noble metals, TCOs and transparent metal nitrides. Reprinted with permission from [67] © The Optical Society. (b) Gap-plasmon resonance calls for particular relationship between the absorption and radiation loss rates, in order to acquire unitary efficiency. Reprinted with permission from [76] © The American Physical Society. (c) Huygens' metasurface supports in-phase electric and magnetic dipoles of the same strength, which results in a unitary transmission and can be directly observed from Smith curves. Reprinted with permission from [77] © John Wiley and Sons. (d) Waveguide-like resonance, enabled by much thicker resonators than those in Huygens' metasurface, can also acquire high transmission at the resonant frequency by carefully engineering the resonant states in it. Reprinted with permission from [78] © Springer Nature.

for transition metal nitrides, a crystalline layer can be grown, so that in spectral range where inter-band loss can be neglected, transition metal nitrides can well replace noble metals. Furthermore, TCOs and nitrides also possess advantages such as property controlling via fabrication [72], CMOS fabrication compatibility, and high stability and tunability [73, 74], which make them popular replacements of noble metals in plasmonics applications. By tuning certain parameters in fabrication process, their plasma frequency can also be changed, which is not possible for noble metals. TCOs can also work as good epsilon-near-zero materials [75], with the real part of its permittivity crossing zero with fairly low loss. Besides, epitaxial silver, owning matched lattice with substrates such as alumina or mica can also refine the grain boundary defects.

In addition to the alternative plasmonic materials, dielectric materials with high refractive indices that support Mie-resonance [79] can also serve as good material candidates for metasurfaces. Dielectric materials have low optical loss and the induced displacement current inside the dielectric nanoparticles can support not only electric multipoles but also magnetic multipoles, which are featured by the circular displacement currents inside the particles [80]. While for plasmonic nanoparticles, magnetic multipoles can only appear with specific structural design, such as split-ring [81] and metal-insulator-metal (MIM) structures [82], due to the vanishing field inside the particles. Besides, Mie resonances can induce a local field enhancement inside the meta-atoms, compared to plasmonic resonance with near surface localization. For the aforementioned reasons, dielectric metasurfaces can exceed plasmonic metasurfaces in several applications, such

as nonlinear devices [18] and directional scattering [83]. Despite all the advantages dielectric materials own compared with plasmonic materials, the size of the meta-atoms and the localized hot spot of the field are much larger due to the considerably smaller permittivity. Silicon [84] and titanium dioxide [85] are prevalently used in near-infrared and visible spectral domain with high and nearly pure real refractive index, which ensure the sufficient enhancement and localization of the field inside the meta-atoms to boost a resonance. Apart from these popular materials, some group IV and group III–V semiconductors, like Ge [86] or GaAs [87], also have the similar response under the incident field.

3.2. *Highly efficient metasurfaces with periodic arrangement*

Besides the inherent material properties, the structure of meta-atoms also plays an important role in efficiency. For metasurfaces with periodic arrangement, several special structures can obtain near unity efficiency at its resonant frequency. For example, metasurfaces supporting gap-plasmon resonance [88] can achieve near unity efficiency in reflection at the resonance frequency. This kind of metasurfaces consist of a thin dielectric spacer sandwiched between a thick metal film and an array of subwavelength metallic meta-atoms, which is also called the metal-insulator-metal structures [89]. This configuration has once attracted a lot of attention due to its simple fabrication yet huge capability of field transformation. This distinctive configuration supports asymmetrically induced conductive current in the upper metallic resonator and the metallic substrate, which can be seen as a transverse magnetic dipole. Different works concerning gap-plasmon resonances exhibited quite different functionalities, ranging from perfect absorber [90] to phase modulation with high reflection [91]. This difference has been clearly explained [76] using coupled-mode theory. When there is only one mode inside the interested spectral range, the periodic gap-plasmon metasurface can be regarded as a one-port single mode resonator. Unity transmission together with a 2π phase delay around resonance occurs as long as the absorptive quality factor is much larger than the radiative quality factor. Different geometrical parameters of MIM structures give different relationships between the absorption loss and radiation loss, which incur the aforementioned various performances from similar MIM structures. For a transmissive platform with two ports, a single mode resonator is not sufficient any more to achieve unitary efficiency at resonant frequency.

Dielectric transmission metasurfaces with periodic arrangement can acquire unity efficiency through two different methods, i.e. the directional scattering and the waveguide-like resonances. The scattering field in meta-atoms can be divided into the superposition of various multipoles [92], so that each meta-atom can be replaced by its equivalent multipoles. When the meta-atom can be regarded as a transverse electric dipole and a magnetic dipole with the same strength and phase, there will be no reflection because of the destructive interference between the scattering fields of these two dipoles. Meanwhile, if the material is lossless, all power will be transmitted and a so-called Kerker effect emerges. This kind of metasurfaces are called Huygens' metasurfaces [77]. The required relationships between the two dipoles are often achieved by embedding cylindrical meta-atoms in a medium with about 1.45 refractive index, which results in a stronger collective interaction in the periodic arrays. Therefore, with a slight change in period or incident angle of the Huygens' metasurface, a large difference in its performance may appear. Different from Huygens' metasurface, which only supports dipole resonances in its composing meta-atoms, metasurfaces with thicker meta-atoms can support waveguide-like resonances [78]. This kind of meta-atoms are usually seen as truncated waveguides supporting Fabry–Perot resonances, which interfere with each other and can lead to a high transmission. The multiple resonant states make it possible to direct all power into the transmitted channel.

3.3. *Highly efficient metasurfaces with spatially-variant meta-atoms*

One distinctive feature of metasurfaces is that they allow for spatial-variant transformation towards incident electromagnetic field [51]. When meta-atoms are arranged in a subwavelength lattice, deliberately design can impart abrupt transformation with subwavelength resolution. One important application of the spatially-variant metasurfaces is beam steering, such as focusing, deflecting, and imaging. The boost in this field occurs when the generalized Snell's law is proposed. Metasurface enables an unprecedented era of interface engineering. Its inhomogeneous trait brings phase delay variations depending on location to compensate the phase difference between incident and desired propagation phase profiles. Considering the conservation of momentum, the phase gradient incurred by the spatial-variant meta-atoms will endow extra terms in conventional Snell's law, which helps achieve extraordinary wave manipulation effects like anomalous refraction [93]. The generalized Snell's law implies the probability of arbitrary modulating of the reflected/transmitted light, where its propagating direction does not have to be located inside the incident-plane and can have nearly arbitrary angle. Enlightened by the generalized Snell's law, numerous work ranging from meta-lens, spin-orbital interaction to holograms, and polarizer have been exhibited. The common process of fulfilling a metasurface with spatially-variant properties starts from finding a set of meta-atoms, which ideally can yield different phase delays covering the full 2π range with unit efficiency in the concerned field (transmitted, reflected or scattered field depending on the specific scene). A simple arrangement of this set of meta-atoms satisfy the phase delay profile indicated by the generalized Snell's Law. Based on these methods, meta-lenses and holograms enabled by metasurfaces can all be obtained with efficiencies as high as 80% or so. However, when it comes to extreme wave manipulations like large angle steering, metasurfaces designed by this strategy is limited in efficiency and may eventually not exhibit the desired performance. This is because of the ignorance of impedance matching between the impinging and desired wave fronts, which is inevitable in beam deflecting and is expected to grow for steeper angles.

By considering the beam steering process, the required transformation imparted by a metasurface can be defined by the establishment of a transversely averaged yet inhomogeneous impedance boundary connecting both the impinging field and the desired field. When the induced currents in the metasurface form the exact impedance, perfect wave manipulation appears with unitary power efficiency. This ideal impedance boundary endowed by the metasurface is different from the phase compensation profile defined by the generalized Snell's Law [23,64], which only considers the locally linear momentum conservation with the spatially-variant phase delay requirements. Impedance matching, however, provides a more comprehensive perspective and sets the ideal local profile in both phase and amplitude of the scattering field radiated from the metasurfaces. Furthermore, the difference of target profiles defined by these two methodologies not only lies in the absent amplitude profiles defined by the generalized Snell's Law, but also in the phase profiles. By taking reflected beam deflection performance as an example, the ideal phase profile defined by impedance matching calls for nonlinear distribution along the metasurface, while the generalized Snell's Law indicates a linear phase gradient, as shown in Figure 4(a). The difference of these two phase profiles becomes larger with the increase of the steering angle and the nonlinear gradient defined by the boundary conditions becomes steeper. This quickly varied nonlinear phase profile requires extremely small discretization and will eventually be limited by the resolution coming from both the size of meta-atoms and the fabrication. Besides, perfect impedance boundary conditions ask for an amplitude profile with both local power absorption and gain oscillations, which may bring tremendous difficulties in involving active meta-atoms. Luckily, these two barriers can be bypassed using merely passive lossless metasurfaces with deliberate consideration.

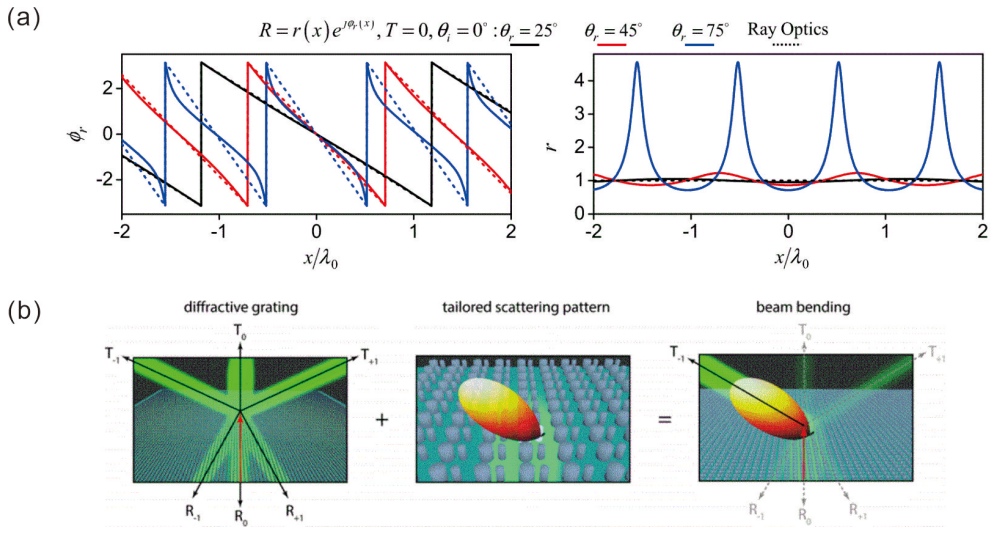

Figure 4. (a) The local reflectance deviation of the profiles defined by the generalized Snell's Law and the impedance boundary conditions in a reflective angle-deflecting metasurfaces, indicated by the dashed and solid lines, respectively. The differences become larger for steeper angle deflection and the unitary efficiency calls for local power absorption and gain oscillations. Reprinted with permission from [23] © The American Physical Society. (b) Concept of a meta-grating. The super lattice determines the diffraction angle, and the inclusions inside the super lattice determines the power rerouting directions. When the inclusions can reroute all the power into one diffraction order, a metasurface can acquire unitary efficiency even in steep angle steering. Reprinted with permission from [94] © The American Chemical Society.

Guided by the impedance boundary conditions, situations in reflection and refraction modes naturally bear large difference. Ideal transmission manipulation can be achieved by passive lossless metasurface, although there are still certain requirements on, for example, bianisotropy [95]. The transmission type metasurface should be reciprocal and allows bianisotropic response with the coupling between electric and magnetic polarizations in a unit cell. Moreover, the coupling coefficient has to be constant depending only on the incident and desired fields, while the electric and magnetic polarizabilities have to be spatially variant and satisfy certain relationships. For reflective metasurfaces, local power absorption and gain oscillations are required to achieve unitary efficiency, where spatial dispersion must be applied for passive metasurfaces [96]. Spatial dispersion makes the perfect reflection with unitary efficiency possible, by allowing periodic flow of power to enter the metasurface and then to launch back. However, this calls for strong nonlocal effect [64] to become locally absorptive and active yet overall passive and global lossless, which is a nontrivial work. A more preferable alternative may be a reflective metasurface allowing the discard of local active part at the cost of low power loss. People find that this part of energy loss is smaller when it reroutes to undesired reflection angle than being absorbed [23]. Therefore, the trade-off strategy is allowing suppressed reflection into undesired direction using lossless reflective metasurfaces. A much better efficiency is acquired in this circumstance than the passive lossy scene with only one desired deflected angle. This strategy also calls for both electric and magnetic polarization to obtain a higher efficiency.

In addition to the satisfactory local amplitude profile, the acquirement of the fast varying phase profile is inherently limited by the pixelate feature of metasurface, which is usually com-

posed of subwavelength lattice. Methods that can surmount the small pixel barrier are highly desired. Meta-grating [63] is a new concept aiming at breaking the limited pixel resolution and offering an utterly continuous phase profile in the super lattice. By using the concept of grating to funnel power into specific channels, the super lattice is a fundamental periodic composition of metasurface and offers continuous transformation by regarding the structure inclusions as a whole. The super lattice selects the desired steering angle as a diffraction order and the complex inclusions inside the super lattice are tailored to reroute the incident power to the desired diffraction order and to suppress the other undesired diffraction orders. This strategy is distinguishable from discretization of the averaged continuous impedance profile, which is inherently limited by the subwavelength fabrication resolution. With meta-gratings, unitary efficiency can be achieved. Special attention should be paid to the complex inclusions in super lattice. For normal incidence, only one Floquet mode funneling power implies the asymmetric scattering by the inclusions, which might be obtained by directional scattering antennas. Various applications apply the metagrating concepts and yield high efficiency and great performance in high NA focusing [97], steep angle deflection [94, 98], etc.

4. Conclusion

Metasurfaces, featured with ultrathin thickness, subwavelength resolution transformation to the wavefront, and diverse interactions with the incident field, serve as a class of unprecedented compact and versatile platforms to modulate the incident electromagnetic waves. The resonances of meta-atoms guarantee their strong interactions with the impinging field, which results in desired transformation within a subwavelength scale. However, separate resonances may bring some inherent limitations, which results in certain restrictions on the properties of temporal dispersion and efficiency of metasurfaces. During the past decade, fruitful works have been done to break these limitations, which further broaden the capabilities of metasurfaces and endow more practical potentials for metasurface applications. These breakthroughs and improvements of metasurfaces come from the exploration and deeper comprehension of novel and multiplicate interactions between meta-atoms and the impinging field. The engineering and exploitation of different kinds of resonances and the control of coupling between them still need further exploration to acquire general guidelines for designing the inclusions and arrangements of metasurfaces.

Besides passive metasurfaces, tunable metasurfaces [99] enabling real-time modulation of both the transmittance/reflectance and phase are also worth being explored. Tunable metasurfaces have great potential in many practical applications such as beam steering in light detection and ranging (LIDAR) and holographic display, where the dispersion engineering and efficiency management are also essential. With these efforts, the capabilities and applications of metasurfaces may be further boosted.

Acknowledgements

National Natural Science Foundation of China (Projects No. 61775113 and No. 11474180).

References

[1] C. Tiejun, D. Smith, L. Ruopeng, *Metamaterials: Theory, Design and Applications*, Springer, New York, 2010.
[2] D. R. Smith, J. B. Pendry, M. C. Wiltshire, "Metamaterials and negative refractive index", *Science* **305** (2004), no. 5685, p. 788-792.
[3] V. M. Shalaev, "Optical negative-index metamaterials", *Nat. Photon.* **1** (2007), no. 1, p. 41.

[4] A. Poddubny, I. Iorsh, P. Belov, Y. Kivshar, "Hyperbolic metamaterials", *Nat. Photon.* **7** (2013), no. 12, p. 948.
[5] D. Schurig, J. Mock, B. Justice, S. A. Cummer, J. B. Pendry, A. Starr, D. Smith, "Metamaterial electromagnetic cloak at microwave frequencies", *Science* **314** (2006), no. 5801, p. 977-980.
[6] A. V. Kildishev, A. Boltasseva, V. M. Shalaev, "Planar photonics with metasurfaces", *Science* **339** (2013), no. 6125, article no. 1232009.
[7] H. T. Chen, A. J. Taylor, N. Yu, "A review of metasurfaces: physics and applications", *Rep. Prog. Phys.* **79** (2016), no. 7, article no. 076401.
[8] X. Song, L. Huang, C. Tang, J. Li, X. Li, J. Liu, Y. Wang, T. Zentgraf, "Selective diffraction with complex amplitude modulation by dielectric metasurfaces", *Adv. Opt. Mater.* **6** (2018), no. 4, article no. 1701181.
[9] A. E. Minovich, A. E. Miroshnichenko, A. Y. Bykov, T. V. Murzina, D. N. Neshev, Y. S. Kivshar, "Functional and nonlinear optical metasurfaces", *Laser Photon. Rev.* **9** (2015), no. 2, p. 195-213.
[10] S. Chen, Z. Li, Y. Zhang, H. Cheng, J. Tian, "Phase manipulation of electromagnetic waves with metasurfaces and its applications in nanophotonics", *Adv. Opt. Mater.* **6** (2018), no. 13, article no. 1800104.
[11] R. Zhao, L. Huang, C. Tang, J. Li, X. Li, Y. Wang, T. Zentgraf, "Nanoscale polarization manipulation and encryption based on dielectric metasurfaces", *Adv. Opt. Mater.* **6** (2018), no. 19, article no. 1800490.
[12] E. Karimi, S. A. Schulz, I. De Leon, H. Qassim, J. Upham, R. W. Boyd, "Generating optical orbital angular momentum at visible wavelengths using a plasmonic metasurface", *Light: Sci. Appl.* **3** (2014), no. 5, article no. e167.
[13] C. L. Holloway, E. F. Kuester, J. A. Gordon, J. O'Hara, J. Booth, D. R. Smith, "An overview of the theory and applications of metasurfaces: the two-dimensional equivalents of metamaterials", *IEEE Antennas Propag. Mag.* **54** (2012), no. 2, p. 10-35.
[14] E. F. Kuester, M. A. Mohamed, M. Piket-May, C. L. Holloway, "Averaged transition conditions for electromagnetic fields at a metafilm", *IEEE Trans. Antennas Propag.* **51** (2003), no. 10, p. 2641-2651.
[15] Y. Yang, A. E. Miroshnichenko, S. V. Kostinski, M. Odit, P. Kapitanova, M. Qiu, Y. S. Kivshar, "Multimode directionality in all-dielectric metasurfaces", *Phys. Rev. B* **95** (2017), no. 16, article no. 165426.
[16] M. A. Kats, N. Yu, P. Genevet, Z. Gaburro, F. Capasso, "Effect of radiation damping on the spectral response of plasmonic components", *Opt. Express* **19** (2011), no. 22, p. 21748-21753.
[17] A. Forouzmand, M. M. Salary, S. Inampudi, H. Mosallaei, "A tunable multigate indium-tin-oxide-assisted all-dielectric metasurface", *Adv. Opt. Mater.* **6** (2018), no. 7, article no. 1701275.
[18] Y. Yang, W. Wang, A. Boulesbaa, I. I. Kravchenko, D. P. Briggs, A. Puretzky, D. Geohegan, J. Valentine, "Nonlinear fano-resonant dielectric metasurfaces", *Nano Lett.* **15** (2015), no. 11, p. 7388-7393.
[19] S. Colburn, A. Zhan, A. Majumdar, "Metasurface optics for full-color computational imaging", *Sci. Adv.* **4** (2018), no. 2, article no. eaar2114.
[20] D. Wen, F. Yue, G. Li, G. Zheng, K. Chan, S. Chen, M. Chen, K. F. Li, P. W. H. Wong, K. W. Cheah, "Helicity multiplexed broadband metasurface holograms", *Nat. Commun.* **6** (2015), p. 8241.
[21] X. Ding, F. Monticone, K. Zhang, L. Zhang, D. Gao, S. N. Burokur, A. de Lustrac, Q. Wu, C. Qiu, A. Alù, "Ultrathin Pancharatnam–Berry metasurface with maximal cross-polarization efficiency", *Adv. Mater.* **27** (2015), no. 7, p. 1195-1200.
[22] G. V. Naik, V. M. Shalaev, A. Boltasseva, "Alternative plasmonic materials: beyond gold and silver", *Adv. Mater.* **25** (2013), no. 24, p. 3264-3294.
[23] N. Mohammadi Estakhri, A. Alù, "Wave-front transformation with gradient metasurfaces", *Phys. Rev. X* **6** (2016), no. 4, article no. 041008.
[24] Y. Yang, I. Kravchenko, D. P. Briggs, J. Valentine, "All-dielectric metasurface analogue of electromagnetically induced transparency", *Nat. Commun.* **5** (2014), p. 5753.
[25] B. Luk'yanchuk, N. I. Zheludev, S. A. Maier, N. J. Halas, P. Nordlander, H. Giessen, C. T. Chong, "The fano resonance in plasmonic nanostructures and metamaterials", *Nat. Mater.* **9** (2010), no. 9, p. 707-715.
[26] U. Fano, "Effects of configuration interaction on intensities and phase shifts", *Phys. Rev.* **124** (1961), no. 6, p. 1866.
[27] A. E. Miroshnichenko, S. Flach, Y. S. Kivshar, "Fano resonances in nanoscale structures", *Rev. Mod. Phys.* **82** (2010), no. 3, p. 2257.
[28] A. Rau, "Perspectives on the fano resonance formula", *Phys. Scr.* **69** (2004), no. 1, article no. C10.
[29] C. W. Hsu, B. Zhen, A. D. Stone, J. D. Joannopoulos, M. Soljačić, "Bound states in the continuum", *Nat. Rev. Mater.* **1** (2016), no. 9, article no. 16048.
[30] K. Koshelev, S. Lepeshov, M. Liu, A. Bogdanov, Y. Kivshar, "Asymmetric metasurfaces with high-q resonances governed by bound states in the continuum", *Phys. Rev. Lett.* **121** (2018), no. 19, article no. 193903.
[31] D. R. Abujetas, N. van Hoof, S. ter Huurne, J. G. Rivas, J. A. Sánchez-Gil, "Spectral and temporal evidence of robust photonic bound states in the continuum on terahertz metasurfaces", *Optica* **6** (2019), no. 8, p. 996-1001.
[32] Y. He, G. Guo, T. Feng, Y. Xu, A. E. Miroshnichenko, "Toroidal dipole bound states in the continuum", *Phys. Rev. B* **98** (2018), article no. 161112.
[33] F. Monticone, A. Alù, "Bound states within the radiation continuum in diffraction gratings and the role of leaky modes", *New J. Phys.* **19** (2017), no. 9, article no. 093011.

[34] M. Liu, D. Y. Choi, "Extreme Huygens' metasurfaces based on quasi-bound states in the continuum", *Nano Lett.* **18** (2018), no. 12, p. 8062-8069.
[35] S. Campione, S. Liu, L. I. Basilio, L. K. Warne, W. L. Langston, T. S. Luk, J. R. Wendt, J. L. Reno, G. A. Keeler, I. Brener, "Broken symmetry dielectric resonators for high quality factor fano metasurfaces", *ACS Photon.* **3** (2016), no. 12, p. 2362-2367.
[36] K. Fan, I. V. Shadrivov, W. J. Padilla, "Dynamic bound states in the continuum", *Optica* **6** (2019), no. 2, p. 169-173.
[37] C. Cui, C. Zhou, S. Yuan, X. Qiu, L. Zhu, Y. Wang, Y. Li, J. Song, Q. Huang, Y. Wang, C. Zeng, J. Xia, "Multiple fano resonances in symmetry-breaking silicon metasurface for manipulating light emission", *ACS Photon.* **5** (2018), no. 10, p. 4074-4080.
[38] S. Romano, G. Zito, S. Torino, G. Calafiore, E. Penzo, G. Coppola, S. Cabrini, I. Rendina, V. Mocella, "Label-free sensing of ultralow-weight molecules with all-dielectric metasurfaces supporting bound states in the continuum", *Photon. Res.* **6** (2018), no. 7, p. 726-733.
[39] Y. K. Srivastava, M. Manjappa, L. Cong, W. Cao, I. Al-Naib, W. Zhang, R. Singh, "Ultrahigh-qfano resonances in terahertz metasurfaces: strong influence of metallic conductivity at extremely low asymmetry", *Adv. Opt. Mater.* **4** (2016), no. 3, p. 457-463.
[40] A. S. Kupriianov, Y. Xu, A. Sayanskiy, V. Dmitriev, Y. S. Kivshar, V. R. Tuz, "Metasurface engineering through bound states in the continuum", *Phys. Rev. Appl.* **12** (2019), no. 1, article no. 014024.
[41] A. Tittl, A. Leitis, M. Liu, F. Yesilkoy, D.-Y. Choi, D. N. Neshev, Y. S. Kivshar, H. Altug, "Imaging-based molecular barcoding with pixelated dielectric metasurfaces", *Science* **360** (2018), no. 6393, p. 1105-1109.
[42] H. Friedrich, D. Wintgen, "Interfering resonances and bound states in the continuum", *Phys. Rev. A* **32** (1985), no. 6, p. 3231.
[43] S. Fan, W. Suh, J. D. Joannopoulos, "Temporal coupled-mode theory for the fano resonance in optical resonators", *JOSA A* **20** (2003), no. 3, p. 569-572.
[44] J. Wiersig, "Formation of long-lived, scarlike modes near avoided resonance crossings in optical microcavities", *Phys. Rev. Lett.* **97** (2006), no. 25, article no. 253901.
[45] A. Kodigala, T. Lepetit, Q. Gu, B. Bahari, Y. Fainman, B. Kante, "Lasing action from photonic bound states in continuum", *Nature* **541** (2017), no. 7636, p. 196-199.
[46] A. A. Bogdanov, K. L. Koshelev, P. V. Kapitanova, M. V. Rybin, S. A. Gladyshev, Z. F. Sadrieva, K. B. Samusev, Y. S. Kivshar, M. F. Limonov, "Bound states in the continuum and fano resonances in the strong mode coupling regime", *Adv. Photon.* **1** (2019), no. 01, article no. 016001.
[47] S. Wang, P. C. Wu, V. C. Su, Y. C. Lai, C. Hung Chu, J. W. Chen, S. H. Lu, J. Chen, B. Xu, C. H. Kuan, T. Li, S. Zhu, D. P. Tsai, "Broadband achromatic optical metasurface devices", *Nat. Commun.* **8** (2017), no. 1, p. 187.
[48] O. Avayu, E. Almeida, Y. Prior, T. Ellenbogen, "Composite functional metasurfaces for multispectral achromatic optics", *Nat. Commun.* **8** (2017), p. 14992.
[49] E. Arbabi, A. Arbabi, S. M. Kamali, Y. Horie, A. Faraon, "Multiwavelength metasurfaces through spatial multiplexing", *Sci. Rep.* **6** (2016), p. 32803.
[50] Z.-B. Fan, H.-Y. Qiu, H.-L. Zhang, X.-N. Pang, L.-D. Zhou, L. Liu, H. Ren, Q.-H. Wang, J.-W. Dong, "A broadband achromatic metalens array for integral imaging in the visible", *Light: Sci. Appl.* **8** (2019), no. 1, p. 67.
[51] D. Lin, P. Fan, E. Hasman, M. L. Brongersma, "Dielectric gradient metasurface optical elements", *Science* **345** (2014), no. 6194, p. 298-302.
[52] M. Khorasaninejad, W. T. Chen, R. C. Devlin, J. Oh, A. Y. Zhu, F. Capasso, "Metalenses at visible wavelengths: diffraction-limited focusing and subwavelength resolution imaging", *Science* **352** (2016), no. 6290, p. 1190-1194.
[53] W. T. Chen, A. Y. Zhu, V. Sanjeev, M. Khorasaninejad, Z. Shi, E. Lee, F. Capasso, "A broadband achromatic metalens for focusing and imaging in the visible", *Nat. Nanotechnol.* **13** (2018), no. 3, p. 220-226.
[54] M. Khorasaninejad, F. Aieta, P. Kanhaiya, M. A. Kats, P. Genevet, D. Rousso, F. Capasso, "Achromatic metasurface lens at telecommunication wavelengths", *Nano Lett.* **15** (2015), no. 8, p. 5358-5362.
[55] E. Arbabi, A. Arbabi, S. M. Kamali, Y. Horie, A. Faraon, "Multiwavelength polarization-insensitive lenses based on dielectric metasurfaces with meta-molecules", *Optica* **3** (2016), no. 6, p. 628-633.
[56] Y. Zhou, I. Kravchenko, H. Wang, J. R. Nolen, G. Gu, J. Valentine, "Multilayer noninteracting dielectric metasurfaces for multiwavelength metaoptics", *Nano Lett.* **18** (2018), no. 12, p. 7529-7537.
[57] S. Wang, P. C. Wu, V. C. Su, Y. C. Lai, M. K. Chen, H. Y. Kuo, B. H. Chen, Y. H. Chen, T. T. Huang, J. H. Wang, R. M. Lin, C. H. Kuan, T. Li, Z. Wang, S. Zhu, D. P. Tsai, "A broadband achromatic metalens in the visible", *Nat. Nanotechnol.* **13** (2018), no. 3, p. 227-232.
[58] E. Arbabi, A. Arbabi, S. M. Kamali, Y. Horie, A. Faraon, "Controlling the sign of chromatic dispersion in diffractive optics with dielectric metasurfaces", *Optica* **4** (2017), no. 6, p. 625-632.
[59] F. Ding, Y. Yang, R. A. Deshpande, S. I. Bozhevolnyi, "A review of gap-surface plasmon metasurfaces: fundamentals and applications", *Nanophotonics* **7** (2018), no. 6, p. 1129-1156.
[60] W. Liu, Y. S. Kivshar, "Generalized Kerker effects in nanophotonics and meta-optics", *Opt. Express* **26** (2018), no. 10, p. 13085-13105.

[61] A. Arbabi, Y. Horie, M. Bagheri, A. Faraon, "Dielectric metasurfaces for complete control of phase and polarization with subwavelength spatial resolution and high transmission", *Nat. Nanotechnol.* **10** (2015), no. 11, p. 937-943.
[62] N. Yu, P. Genevet, M. A. Kats, F. Aieta, J. P. Tetienne, F. Capasso, Z. Gaburro, "Light propagation with phase discontinuities: generalized laws of reflection and refraction", *Science* **334** (2011), no. 6054, p. 333-337.
[63] Y. Rad'i, D. L. Sounas, A. Alù, "Metagratings: beyond the limits of graded metasurfaces for wave front control", *Phys. Rev. Lett.* **119** (2017), no. 6, article no. 067404.
[64] A. Díaz-Rubio, V. S. Asadchy, A. Elsakka, S. A. Tretyakov, "From the generalized reflection law to the realization of perfect anomalous reflectors", *Sci. Adv.* **3** (2017), no. 8, article no. e1602714.
[65] E. Hutter, J. H. Fendler, "Exploitation of localized surface plasmon resonance", *Adv. Mater.* **16** (2004), no. 19, p. 1685-1706.
[66] P. B. Johnson, R.-W. Christy, "Optical constants of the noble metals", *Phys. Rev. B* **6** (1972), no. 12, p. 4370.
[67] G. V. Naik, J. Kim, A. Boltasseva, "Oxides and nitrides as alternative plasmonic materials in the optical range [invited]", *Opt. Mater. Express* **1** (2011), no. 6, p. 1090-1099.
[68] S. A. Gregory, Y. Wang, C. De Groot, O. L. Muskens, "Extreme subwavelength metal oxide direct and complementary metamaterials", *ACS Photon.* **2** (2015), no. 5, p. 606-614.
[69] U. Guler, G. V. Naik, A. Boltasseva, V. M. Shalaev, A. V. Kildishev, "Performance analysis of nitride alternative plasmonic materials for localized surface plasmon applications", *Appl. Phys. B* **107** (2012), no. 2, p. 285-291.
[70] U. Guler, A. Boltasseva, V. M. Shalaev, "Refractory plasmonics", *Science* **344** (2014), no. 6181, p. 263-264.
[71] L. Gui, S. Bagheri, N. Strohfeldt, M. Hentschel, C. M. Zgrabik, B. Metzger, H. Linnenbank, E. L. Hu, H. Giessen, "Nonlinear refractory plasmonics with titanium nitride nanoantennas", *Nano Lett.* **16** (2016), no. 9, p. 5708-5713.
[72] Y. Wang, A. Capretti, L. Dal Negro, "Wide tuning of the optical and structural properties of alternative plasmonic materials", *Opt. Mater. Express* **5** (2015), no. 11, p. 2415-2430.
[73] M. Z. Alam, I. De Leon, R. W. Boyd, "Large optical nonlinearity of indium tin oxide in its epsilon-near-zero region", *Science* **352** (2016), no. 6287, p. 795-797.
[74] J. Park, J. H. Kang, S. J. Kim, X. Liu, M. L. Brongersma, "Dynamic reflection phase and polarization control in metasurfaces", *Nano Lett.* **17** (2017), no. 1, p. 407-413.
[75] A. Howes, W. Y. Wang, I. Kravchenko, J. Valentine, "Dynamic transmission control based on all-dielectric Huygens metasurfaces", *Optica* **5** (2018), no. 7, p. 787-792.
[76] C. Qu, S. Ma, J. Hao, M. Qiu, X. Li, S. Xiao, Z. Miao, N. Dai, Q. He, S. Sun, L. Zhou, "Tailor the functionalities of metasurfaces based on a complete phase diagram", *Phys. Rev. Lett.* **115** (2015), no. 23, article no. 235503.
[77] M. Decker, I. Staude, M. Falkner, J. Dominguez, D. N. Neshev, I. Brener, T. Pertsch, Y. S. Kivshar, "High-efficiency dielectric Huygens' surfaces", *Adv. Opt. Mater.* **3** (2015), no. 6, p. 813-820.
[78] A. Arbabi, E. Arbabi, S. M. Kamali, Y. Horie, S. Han, A. Faraon, "Miniature optical planar camera based on a wide-angle metasurface doublet corrected for monochromatic aberrations", *Nat. Commun.* **7** (2016), p. 13682.
[79] A. I. Kuznetsov, A. E. Miroshnichenko, M. L. Brongersma, Y. S. Kivshar, B. Luk'yanchuk, "Optically resonant dielectric nanostructures", *Science* **354** (2016), no. 6314, p. 2956-2963.
[80] N. Papasimakis, V. A. Fedotov, V. Savinov, T. A. Raybould, N. I. Zheludev, "Electromagnetic toroidal excitations in matter and free space", *Nat. Mater.* **15** (2016), no. 3, p. 263-271.
[81] J. Zhou, T. Koschny, C. M. Soukoulis, "Magnetic and electric excitations in split ring resonators", *Opt. Express* **15** (2007), no. 26, p. 17881-17890.
[82] S. Alrasheed, E. Di, "Giant magnetic field enhancement in hybridized mim structures", *IEEE Photon. Technol. Lett.* **29** (2017), no. 24, p. 2151-2154.
[83] I. Staude, A. E. Miroshnichenko, M. Decker, N. T. Fofang, S. Liu, E. Gonzales, J. Dominguez, T. S. Luk, D. N. Neshev, I. Brener, "Tailoring directional scattering through magnetic and electric resonances in subwavelength silicon nanodisks", *ACS Nano* **7** (2013), no. 9, p. 7824-7832.
[84] I. Staude, J. Schilling, "Metamaterial-inspired silicon nanophotonics", *Nat. Photon.* **11** (2017), no. 5, p. 274-284.
[85] R. C. Devlin, M. Khorasaninejad, W. T. Chen, J. Oh, F. Capasso, "Broadband high-efficiency dielectric metasurfaces for the visible spectrum", *Proc. Natl. Acad. Sci. USA* **113** (2016), no. 38, p. 10473-10478.
[86] X. Zhu, W. Yan, U. Levy, N. A. Mortensen, A. Kristensen, "Resonant laser printing of structural colors on high-index dielectric metasurfaces", *Sci. Adv.* **3** (2017), no. 5, article no. e1602487.
[87] S. Liu, M. B. Sinclair, S. Saravi, G. A. Keeler, Y. Yang, J. Reno, G. M. Peake, F. Setzpfandt, I. Staude, T. Pertsch, "Resonantly enhanced second-harmonic generation using iii–v semiconductor all-dielectric metasurfaces", *Nano Lett.* **16** (2016), no. 9, p. 5426-5432.
[88] A. Pors, S. I. Bozhevolnyi, "Plasmonic metasurfaces for efficient phase control in reflection", *Opt. Express* **21** (2013), no. 22, p. 27438-27451.
[89] L. Zhang, S. Mei, K. Huang, C. Qiu, "Advances in full control of electromagnetic waves with metasurfaces", *Adv. Opt. Mater.* **4** (2016), no. 6, p. 818-833.
[90] C. M. Watts, X. Liu, W. J. Padilla, "Metamaterial electromagnetic wave absorbers", *Adv. Mater.* **24** (2012), no. 23, p. OP98-OP120.

[91] G. Zheng, H. Muhlenbernd, M. Kenney, G. Li, T. Zentgraf, S. Zhang, "Metasurface holograms reaching 80% efficiency", *Nat. Nanotechnol.* **10** (2015), no. 4, p. 308-312.
[92] R. Alaee, C. Rockstuhl, I. Fernandez-Corbaton, "An electromagnetic multipole expansion beyond the long-wavelength approximation", *Opt. Commun.* **407** (2018), p. 17-21.
[93] N. Yu, F. Capasso, "Flat optics with designer metasurfaces", *Nat. Mater.* **13** (2014), no. 2, p. 139-150.
[94] E. Khaidarov, H. Hao, R. Paniagua-Dominguez, Y. F. Yu, Y. H. Fu, V. Valuckas, S. L. K. Yap, Y. T. Toh, J. S. K. Ng, A. I. Kuznetsov, "Asymmetric nanoantennas for ultrahigh angle broadband visible light bending", *Nano Lett.* **17** (2017), no. 10, article no. 28898084.
[95] A. Serdiukov, I. Semchenko, S. Tertyakov, A. Sihvola, *Electromagnetics of Bi-anisotropic Materials—Theory and Application, Vol. 11*, Gordon and Breach Science Publishers, 2001.
[96] V. S. Asadchy, M. Albooyeh, S. N. Tcvetkova, A. Díaz-Rubio, Y. Ra'di, S. Tretyakov, "Perfect control of reflection and refraction using spatially dispersive metasurfaces", *Phys. Rev. B* **94** (2016), no. 7, article no. 075142.
[97] R. Paniagua-Dominguez, Y. F. Yu, E. Khaidarov, S. Choi, V. Leong, R. M. Bakker, X. Liang, Y. H. Fu, V. Valuckas, L. A. Krivitsky, "A metalens with a near-unity numerical aperture", *Nano Lett.* **18** (2018), no. 3, p. 2124-2132.
[98] D. Sell, J. Yang, S. Doshay, R. Yang, J. A. Fan, "Large-angle, multifunctional metagratings based on freeform multimode geometries", *Nano Lett.* **17** (2017), no. 6, p. 3752-3757.
[99] T. Cui, B. Bai, H. Sun, "Tunable metasurfaces based on active materials", *Adv. Funct. Mater.* **29** (2019), no. 10, article no. 1806692.